Available online at www.sciencedirect.com

SCIENCE DIRECT®

ELSEVIER

Earth and Planetary Science Letters 211 (2003) 13–26

EPSL

www.elsevier.com/locate/epsl

# A case for a comet impact trigger for the Paleocene/Eocene thermal maximum and carbon isotope excursion

D.V. Kent [a,b,*], B.S. Cramer [a,c], L. Lanci [a,d], D. Wang [e], J.D. Wright [a], R. Van der Voo [e]

[a] *Department of Geological Sciences, Rutgers University, Piscataway, NJ 08854, USA*
[b] *Lamont-Doherty Earth Observatory, Palisades, NY 10964, USA*
[c] *Institute of Geology and Paleontology, Tohoku University, Sendai 980-8578, Japan*
[d] *Instituto di Dinamica Ambientale, Università di Urbino, 61029 Urbino, Italy*
[e] *Department of Geological Sciences, University of Michigan, Ann Arbor, MI 48109, USA*

Received 25 June 2002; received in revised form 22 March 2003; accepted 31 March 2003

**Abstract**

We hypothesize that the rapid onset of the carbon isotope excursion (CIE) at the Paleocene/Eocene boundary (~55 Ma) may have resulted from the accretion of a significant amount of $^{12}$C-enriched carbon from the impact of a ~10 km comet, an event that would also trigger greenhouse warming leading to the Paleocene/Eocene thermal maximum and, possibly, thermal dissociation of seafloor methane hydrate. Indirect evidence of an impact is the unusual abundance of magnetic nanoparticles in kaolinite-rich shelf sediments that closely coincide with the onset and nadir of the CIE at three drill sites on the Atlantic Coastal Plain. After considering various alternative mechanisms that could have produced the magnetic nanoparticle assemblage and by analogy with the reported detection of iron-rich nanophase material at the Cretaceous/Tertiary boundary, we suggest that the CIE occurrence was derived from an impact plume condensate. The sudden increase in kaolinite is thus thought to represent the redeposition on the marine shelf of a rapidly weathered impact ejecta dust blanket. Published reports of a small but significant iridium anomaly at or close to the Paleocene/Eocene boundary provide supportive evidence for an impact.


*Keywords:* Paleocene/Eocene boundary; thermal maximum; PETM; carbon isotope excursion; CIE; comet impact; magnetic nanoparticles; methane hydrate

## 1. Introduction

The Paleocene/Eocene (P/E) boundary (~55 Ma) is marked by an abrupt carbon isotope excursion (CIE) recorded in marine and terrestrial systems (e.g. [1,2]) that is coincident with an equally rapid oxygen isotope excursion interpreted as the P/E thermal maximum [3]. Closely associated with the P/E boundary was the largest deep-sea benthic extinction of the past 90 Myr [4] as well as a major radiation of mammals [5]. A widely accepted explanation for the CIE is the sudden dissociation of $^{12}$C-enriched marine gas

* Corresponding author. Tel.: +1-845-365-8544; Fax: +1-732-445-3374.
*E-mail address:* dvk@rci.rutgers.edu (D.V. Kent).

0012-821X/03/$ – see front matter 
doi:10.1016/S0012-821X(03)00188-2

hydrates [6–8]. Such a major dissociation event would seem to require either a thermal [6] or mechanical [9] precursor. However, high-resolution oxygen and carbon isotope records have yet to demonstrate a significant warming immediately preceding the CIE (e.g. [10–12] despite recent assertions to the contrary [13]; see below) and a geologic event of sufficient magnitude to provide a plausible mechanical trigger has not been identified.

We suggest that the impact of a volatile-rich comet provides an alternative source of $^{12}$C-enriched carbon to account for the rapid onset of the CIE. The massive introduction of carbon directly into the atmosphere would account for the concomitantly rapid greenhouse warming, producing newly corrosive and warmer (and hence less oxygenated) bottom waters that have previously been suggested as proximate causal mechanisms for the massive extinction of benthic organisms coincident with the CIE [1,4]. An impact has been entertained as one of several possible explanations for a small but analytically significant iridium anomaly detected at or very close to the P/E boundary [14,15]. We describe new albeit indirect evidence for an impact at the P/E boundary based on the discovery of abundant magnetic nanoparticles in kaolinitic clays that are closely associated with the CIE in shelf sediments on the Atlantic Coastal Plain.

## 2. Lithologic and magnetic changes at the CIE

The P/E boundary interval was recovered and studied in a transect of three drill cores across the Atlantic Coastal Plain in New Jersey – at Bass River [16,17], Ancora [18,19] and Clayton [20] (Fig. 1). Published biostratigraphic and magnetostratigraphic data for the Bass River core indicate that the negative excursion in the carbon isotopic composition of carbonates corresponds to the CIE [16,17], whose onset is now taken to coincide with the P/E boundary at around 55 Ma [21]. We found a correlative CIE in the Ancora and Clayton cores (Fig. 2). The stratigraphic records across the CIE are not interrupted by sequence boundaries and appear to be complete.

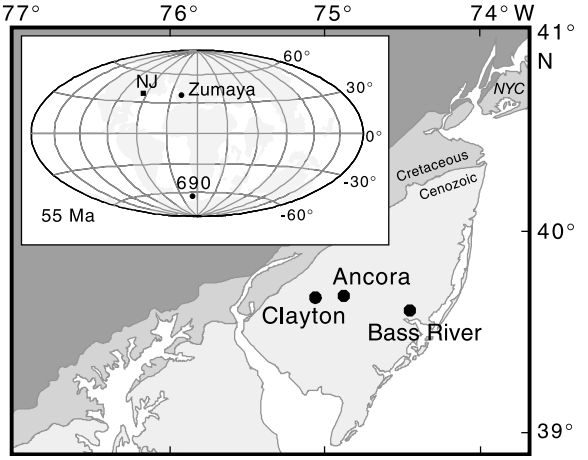


Fig. 1. Location map for Ancora [18], Bass River [16] and Clayton [20] drill sites on the Atlantic Coastal Plain of New Jersey where the CIE interval was investigated in this study. Inset shows locations on a 55 Ma plate reconstruction sketch map of some other CIE sites discussed in the text.

The CIE interval in this neritic setting is closely associated with a several meters thick clay-rich unit in which the proportion of kaolinite becomes significantly higher and terrigenous sand is conspicuously absent [17,20] (Fig. 2). Intervals relatively enriched in kaolinite have been documented coincident with the CIE in shelf sediments around the Tethys [22] and in New Zealand [8], and in deep-sea sediments from the Southern Ocean [23]. Kaolinite is the product of intensive continental weathering, generally under hot, humid conditions over appreciable time scales ($10^5$–$10^6$ yr [24]). However, the close correspondence of the kaolinite-rich interval with minimum carbon isotope values (Fig. 2) indicates that this unit was deposited very rapidly. In open ocean sections, such minimum carbon isotope values occur over an interval of a few decimeters at most [12], suggesting that the onset and nadir of the CIE occurred over time scales of only $< 10^3$–$10^4$ yr [25]). We therefore conclude that the CIE clay unit at the New Jersey P/E boundary sections was deposited at rates exceeding 30–70 cm/kyr. This is consistent with the presence throughout this interval in the New Jersey sections of calcareous nannoplankton and planktonic foraminiferal taxa that are restricted to the early part of the CIE interval at other locations [18,26–29].

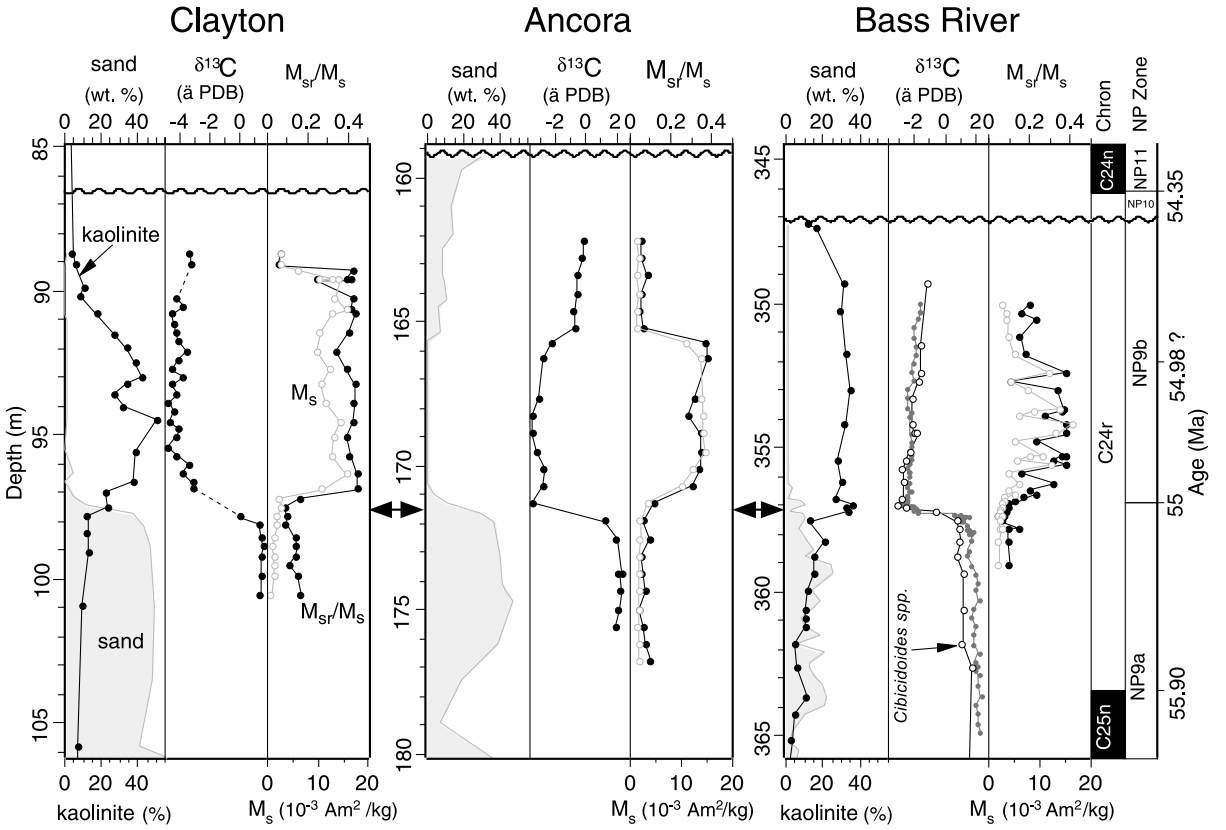


Fig. 2. Lithologic, isotopic and magnetic hysteresis profiles across the CIE interval in three drill cores on the Atlantic Coastal Plain of New Jersey (see Fig. 1 for locations). Double-arrows mark the onset of the CIE interval. Magnetostratigraphic, biostratigraphic, lithologic and benthic foraminiferal isotopic data for Bass River are from [17], lithologic data for Clayton from [20]. The sand-fraction record does not differentiate between largely quartz and glauconite sand below the CIE and exclusively biogenic (e.g. foraminiferal) sand within the CIE interval. Bulk carbonate carbon isotope data were generated for this study. Samples for carbon isotope analysis were ground and reacted in phosphoric acid ($H_3PO_4$) at 90°C in a Multiprep system attached to a Micromass Optima mass spectrometer. The close correspondence between bulk carbonate and benthic foraminiferal $\delta^{13}C$ records at Bass River indicates that the bulk carbonate $\delta^{13}C$ records accurately reflect local seawater-dissolved inorganic carbon at the time of deposition. The magnitude of the $\delta^{13}C$ decrease recorded in these sections (−4 to −5‰) is substantially larger than that recorded in deep-sea records, but is similar to the atmospheric/surface-ocean records of surface-dwelling planktonic foraminifera [1,13] and terrestrial carbonates [2,59]. Saturation magnetization ($M_s$) and the ratio of saturation remanence to saturation magnetization ($M_{sr}/M_s$) were determined from hysteresis measurements on ~20 mg bulk sediment samples (see Fig. 3).

Sediment magnetization was studied by low field susceptibility and magnetic hysteresis properties and the magnetic mineralogy was constrained from analyses of remanent magnetic coercivity from backfield IRM curves. Anomalously highly magnetized sediments were initially discovered in a 6.5 m thick interval uniquely associated with the CIE in a core-log integration study of middle Miocene to Cenomanian coastal plain strata at the Ancora site [18,19]. New magnetic hysteresis data (Fig. 3a,b) substantiate this observation at the Bass River and Clayton sites where we find that sediments associated with the CIE from a 4.6 m thick interval at Bass River and a 7.6 m thick interval at Clayton are also characterized by $M_s$ intensities of around 15 mA $m^2$/kg, an order of magnitude greater than in the underlying or overlying sediments (Fig. 2). More significantly, high $M_{sr}/M_s$ ratios averaging 0.40 at the more proximal (landward) Clayton site, 0.35 at Ancora,

and 0.3 with more variability at the more distal Bass River site are associated with the high magnetizations in the CIE interval. Backfield IRM curves in the highly magnetized CIE sediments approach saturation by about 200 mT (Fig. 3c), suggesting that the main magnetic mineral is magnetite or possibly a partially oxidized form of maghemite. The high magnetizations correspond to volumetric concentrations of about 100 parts per million for such magnetic particles. High-field heating experiments to determine Curie temperatures were not successful due to the creation of a magnetic alteration phase presumably from breakdown of clays although we can say there was no initial magnetic phase with a Curie temperature lower than about 450°C. Samples from outside the CIE interval (or some samples within the CIE at Bass River) that have reduced $M_{sr}/M_s$ may not reach saturation by 1000 mT, indicating the presence of a more highly coercive mineral like goethite or hematite in these samples.

Experimental data [30] and theory [31,32] show that, unless elongated, magnetite grains have a very narrow stable single domain size range where $M_{sr}/M_s$ is high only between the superparamagnetic threshold of 30–50 nm and the multidomain threshold of about 70–100 nm. For example, the average $M_{sr}/M_s$ for randomly oriented, non-interacting cuboid magnetite grains is calculated to drop precipitously from 0.40 for 90 nm grains to multidomain-like values of 0.06 for 104 nm grains [32]. This means that the presence of even relatively few magnetic grains above the multidomain threshold size will tend to lower the overall $M_{sr}/M_s$ ratio of an assemblage because of their disproportionately large volumetric contribution. At the other end of the size spectrum, $M_{sr}/M_s$ will be reduced due to superparamagnetic behavior

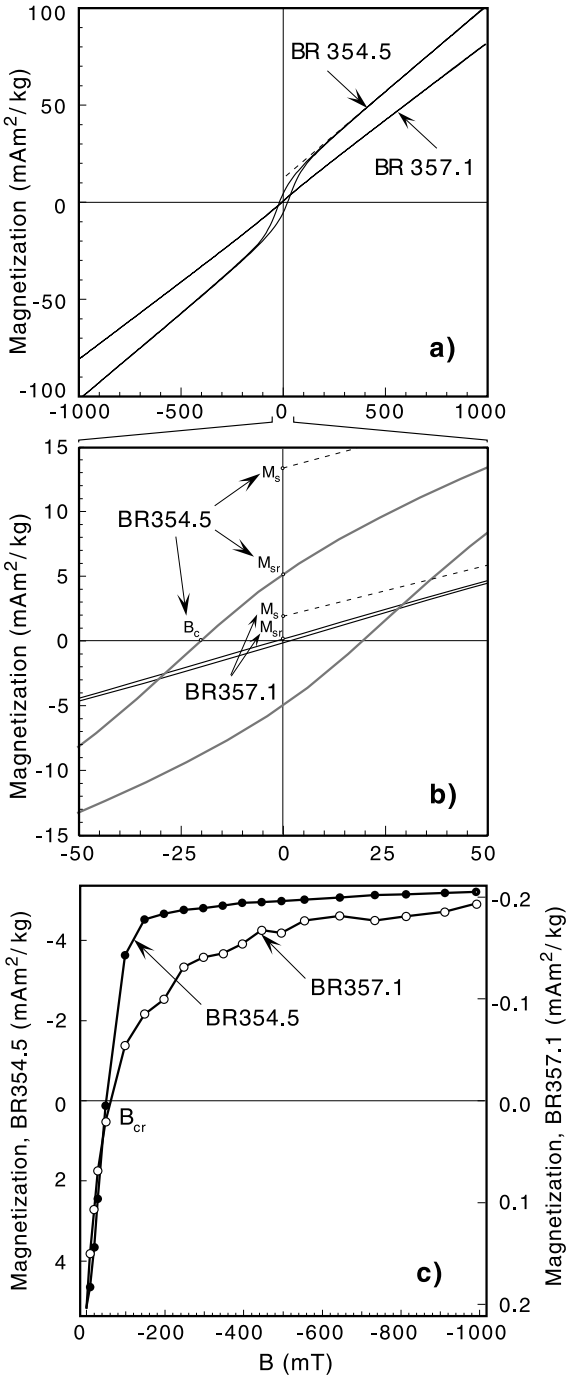


←

Fig. 3. Examples of magnetic hysteresis loops (a, full scale; b, expanded scale) determined on ~20 mg bulk sediment samples from within (BR354.5) and below (BR351.1) the CIE interval in the Bass River drill core. Measurements were made on an alternating-gradient force magnetometer (Micromag 2900) using a maximum field of 1000 mT; $M_s$ is determined after standard correction for the high field paramagnetic slope from 7000 to 1000 mT (shown as dashed line in panels a and b). $M_{sr}/M_s$ is 0.38 for BR354.5 and 0.076 for BR357.1. Magnetic coercivity, $B_c$, is magnetization zero-crossing. Backfield IRM curves used to measure remanent coercivity ($B_{cr}$, zero-crossing or remanent magnetization) are shown in panel c.

[33,34], although the volumetric contribution of such very fine grains to bulk magnetic hysteresis properties will tend to be small.

The high $M_{sr}/M_s$ ratios of the CIE sediments are unusual and not expected to result from an assemblage of detrital magnetic minerals and the heterogeneity of neritic sedimentary processes, especially over several meters of section. A recent compilation of hysteresis data for rocks and sediments [35] shows that $M_{sr}/M_s$ ratios rarely approach 0.4 in magnetite-bearing clastic sediments; for example, pelagic deep-sea sediments [36] have $M_{sr}/M_s$ ratios that range only to about 0.3, whereas Chinese loess and paleosols [37] and many lake sediments (e.g. [38], but see [39]) typically have even lower values (Fig. 4). Some marine limestones, especially those that have been remagnetized [40], do have $M_{sr}/M_s$ ratios that can be as high as those for the CIE sediments. However, such carbonates reflect depositional and diagenetic processes very different from the CIE sediments, making it unlikely that the magnetic mineralogy has a similar origin. Moreover, the sudden change observed at the CIE onset would remain unexplained.

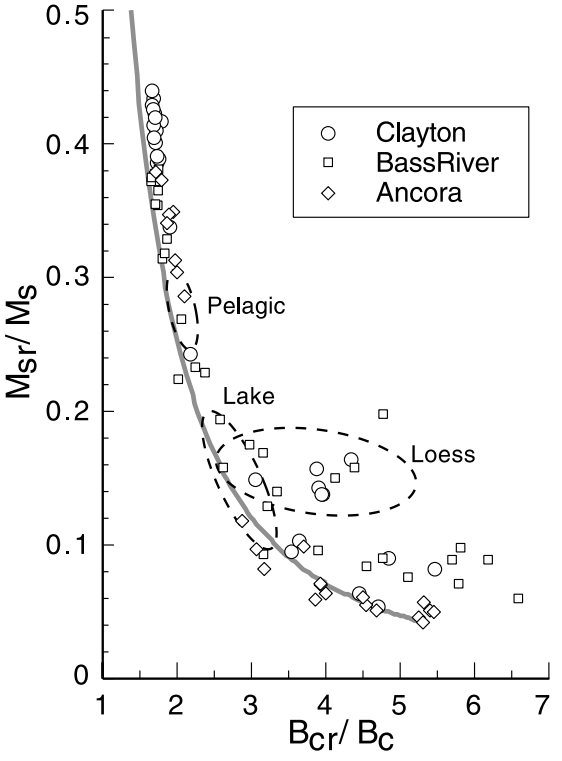


Fig. 4. Day plot of magnetic hysteresis parameters ($M_{sr}/M_s$ versus the ratio of remanent coercivity to coercivity, $B_{cr}/B_c$) for samples from across the CIE interval in the Clayton, Bass River and Ancora drill cores. Shown for comparison are generalized data fields (dashed) for Chinese loess [37], lake sediments [38], and pelagic deep-sea sediments [36] taken from a recent summary [35]. Solid curve is a SD–MD theoretical mixing curve from [35].

## 3. Interpretation of lithologic and magnetic changes at the CIE

We interpret the hysteresis properties of the CIE sediments as indicative of a highly restricted magnetic grain-size assemblage concentrated in the single domain range ($<100$ nm) in the more proximal (landward) Clayton and Ancora sites, with sporadic admixtures of larger multidomain-like particles in the more distal Bass River site. The magnetic nanoparticle assemblage and its depositional pattern are unusual and require explanation. An intriguing possibility that we initially considered [19] is that the magnetic particles are of biogenic origin. This is because magnetotactic bacteria are known to form small magnetite crystals [41] and available hysteresis data indicate that magnetosomes isolated from magnetotactic bacterial cells can have high $M_{sr}/M_s$ values [42]. A transmission electron microscope (TEM) study of a sample from the CIE interval at Clayton shows that iron-rich grains are very difficult to detect and are likely to be very small. Four iron-rich grains have been observed and two were confirmed as magnetite on the basis of their diffraction pattern (Fig. 5). Their grain sizes of $\sim$70 nm are well within the theoretical single domain grain size range, consistent with the hysteresis data. The magnetite grains have equidimensional shapes but they do not occur in strings, which are often indicative of biogenic origin [41]. A biogenic origin would also not account for the apparent exclusion of larger detrital magnetic grains in these neritic deposits even though the updip–downdip gradient in thickness of the CIE clay layer is more consistent with a detrital (landward) source for the magnetic particles.

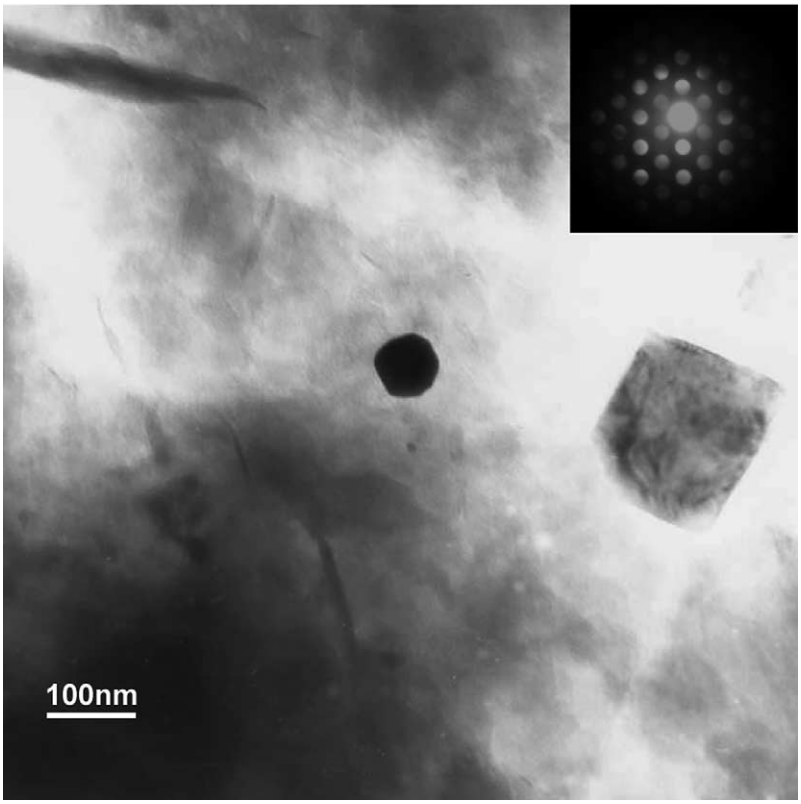


Fig. 5. TEM bright field image of a magnetite grain (dark object in center of field) from a sample at 96.35 m in the CIE interval at Clayton. The sediment sample was ground under ethanol in an agate mortar for several minutes; a droplet of the mixture was then dropped on a copper washer with substrate and coated with carbon. TEM observations were made using a Philips CM12 STEM working at 120 kV. The sparse distribution and small grain size of the iron-rich particles made them extremely difficult to find. The chemical composition was determined using a Kevex EDS detector equipped with the STEM. Convergent beam electron diffraction (CBED) pattern ([011] diffraction) of the grain is shown as inset and is consistent with that of magnetite (F d3m, cubic, $a = \sim 8.4$ Å).

The sudden increase in kaolinite, which coincides with the magnetic nanoparticle assemblage, may be due to the reworking of Upper Cretaceous kaolinites, although there is no obvious mechanism for preferential erosion and redeposition of these deposits [17]. Samples we collected from exposures of the Upper Cretaceous Raritan Formation at Sayreville, NJ, have different magnetic properties with very low $M_{sr}/M_s$ ($\sim 0.04$), indicating that high $M_{sr}/M_s$ values are not characteristic of all kaolinitic deposits. Fine-grained magnetites have been suggested to precipitate near the iron redox boundary in suboxic marine sediments [43], but this process is often followed by dissolution of magnetite by reduction diagenesis lower in the sediment column (e.g. [44,45]) and thus not expected to result in a thick layer rich in fine-grained magnetite. Parenthetically, reported $M_{sr}/M_s$ values of suboxic sediments are only about 0.3, even though magnetotactic bacteria are a likely source of the fine-grained authigenic magnetite [43].

Iron-rich nanophase material has been detected using Mössbauer spectroscopy at several Cretaceous/Tertiary (K/T) boundary sites where, although often in the form of hematite and goethite perhaps due to weathering, it has been interpreted as a condensate from an impact ejecta plume [46,47]. The dominance of magnetic nanoparticles inferred from hysteresis data in the CIE

interval at the three Atlantic Coastal Plain sites may have a similar origin and, if so, provides circumstantial evidence for an impact at the P/E boundary. Rapid nucleation and limited crystal growth during cooling of an expanding plume vapor can account for the absence of larger magnetic grains.

In this scenario, the sudden increase in kaolinite content at the onset of the CIE may have resulted from accelerated weathering of a layer of very fine-grained dust, such as an impact ejecta blanket consisting mainly of crustal material thrown up by the impact. The close correspondence of the kaolinite-rich interval with minimum carbon isotope values (Fig. 2) indicates that this unit was deposited very rapidly, suggesting that the unconsolidated impact dust blanket was rapidly weathered and eroded from the land and redeposited on the continental shelf. Such circumstances could explain the remarkable homogeneity of the magnetic, lithologic, and isotopic properties of these CIE sediments. Rapid weathering, erosion and redeposition of an impact ejecta blanket would also account for the abrupt transition from typical neritic sandy and silty clays below the CIE to kaolinite-rich clays containing very little silt and only non-terrigenous (e.g. foraminiferal) sand-size material just after the onset the CIE, with greatest focusing and least contamination from other sediment sources at the most proximal (Clayton) site.

## 4. Other evidence for an impact

More direct but contentious evidence of an impact event at the P/E boundary is a reproducible albeit small iridium anomaly (quoted values of $143 \pm 22$ ppt and $133 \pm 15$ ppt Ir compared to a background of about 38 ppt Ir) in an expanded bathyal section at Zumaya, Spain [14]. The anomaly occurs in a 1 cm thick gray layer at the base of a $\sim$35 cm thick greenish brown marl and is coincident with the initial $\sim$1‰ decrease in $\delta^{13}C$ values marking the onset of the CIE (Fig. 6a). The iridium enrichment was regarded as enigmatic [14] and could be due to various other causes such as basaltic volcanism [48], although there is no evidence for a volcanic ash layer at

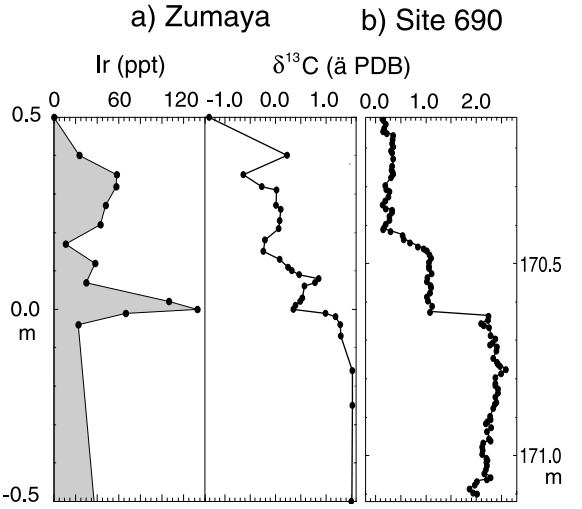


Fig. 6. (a) Profiles of bulk carbonate $\delta^{13}C$ and iridium concentrations across the onset of the CIE recorded in Zumaya, Spain (from figure 2 in [14]). (b) High-resolution profile of bulk carbonate $\delta^{13}C$ across the onset of the CIE from ODP Site 690 from the Southern Ocean (from figure 2 in [12]). Both records are plotted on same linear thickness scale and show a stepped decrease in $\delta^{13}C$ after the initial $-1$‰ shift, which coincides with the iridium anomaly at Zumaya. Note that no intermediate values are resolved in the initial shift at either site, while subsequent steps are more gradual.

this stratigraphic level despite detailed analyses [14]. We view the precise coincidence of the sharp iridium anomaly with the base of the CIE at Zumaya as remarkable and supportive of an impact origin. An iridium anomaly has also been reported more recently from near the P/E boundary in flysch deposits in Slovenia [15], although in the absence of carbon isotope data it is not possible to determine if it coincides with the CIE.

Other geochemical evidence for a P/E impact is more equivocal. If the onset of the CIE was associated with an extraterrestrial impact it might be expected to have low $^{187}Os/^{188}Os$ isotope ratios. Instead, an excursion to higher values of $^{187}Os/^{188}Os$ isotope ratios was found in DSDP Site 549 from the North Atlantic and attributed to a global increase in chemical weathering rates over several hundred thousand years during an interval of unusually warm global climate following the CIE [49]. However, the sampling interval (12 samples over $\sim$400 kyr) was insufficient to capture the rapid onset of the event and the data are

therefore inconclusive regarding the triggering mechanism. As Ravizza et al. [49] point out, in a longer osmium isotope record from North Pacific core GPC3 [50], an osmium isotope *minimum* occurs in an interval that has been correlated with the P/E boundary [51]. We suggest that although the origin of this minimum is highly uncertain [49,50], a contribution from extraterrestrial osmium cannot be excluded.

Core GPC3 also yielded a continuous record of extraterrestrial helium borne by the fallout of interplanetary dust particles over the past 70 Myr [52]. The observation that the K/T boundary, which is identified in these sediments by a large iridium anomaly [53], has no associated peak in extraterrestrial helium can be explained by devolatization of a large body during impact [52]. Accordingly, the absence of a significant increase in extraterrestrial helium at around the P/E boundary [52] does not preclude an impact of a large extraterrestrial object but does suggest that it was not accompanied by a comet shower as inferred for the late Eocene [54].

## 5. Estimate of comet size from carbon isotope evidence

In the absence of any other major source of sufficiently $^{12}C$-enriched carbon, it has been assumed that the CIE resulted from dissociation of seafloor methane hydrate deposits having $\delta^{13}C$ values of about −60‰ [6,7]. However, space probe measurements of Comet Halley show that cometary material is rich in carbon [55,56] with measured $^{12}C/^{13}C$ ratios as high as 5000 compared to terrestrial values of about 89 [56]. Interplanetary dust particles collected in the Earth's atmosphere and thought to represent, at least in part, cometary dust [57] also show $^{12}C$ enrichment and can have $\delta^{13}C$ values of −45‰ or lower [58] (Fig. 7). An impact of a cometary body can therefore provide an alternative source of $^{12}C$-enriched carbon as well as explain the magnetic nanoparticles on the New Jersey shelf and the iridium anomaly at Zumaya.

Assuming a cometary source of $^{12}C$-enriched carbon, the magnitude of the CIE can be used

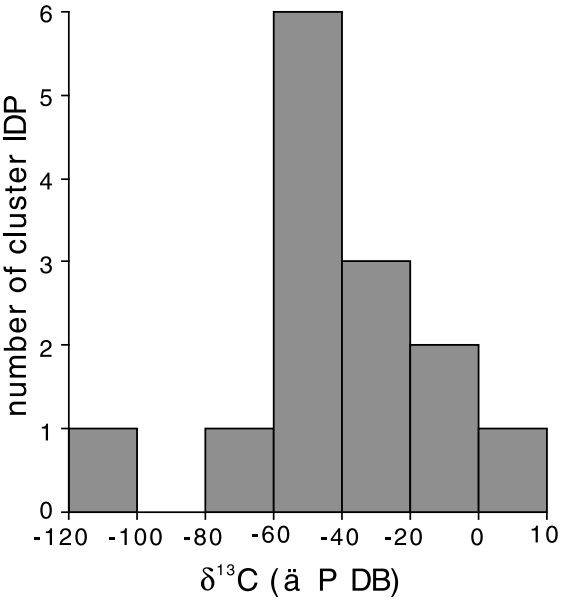


Fig. 7. Histogram of cluster interplanetary dust particle (IDP) $\delta^{13}C$ values (data from [58]).

to estimate the size of the P/E impactor. The CIE is characterized by a stepped decrease in bulk carbonate $\delta^{13}C$ values (Fig. 6a,b), but the initial negative shift of ∼1‰ is significantly more abrupt than subsequent steps and must have occurred in much less than 1000 yr [12]. At most, a comet impact would be called upon to account only for the initial decrease, which we note is coincident with the Ir anomaly at Zumaya [14]. For a cometary body with −45‰ $\delta^{13}C$, ∼900 Gt of extraterrestrial carbon would account for a 1‰ decrease in a total exchangeable carbon reservoir of 40 000 Gt (Fig. 8). A more reasonable estimate is obtained by accounting for a 4‰ shift in only the surface ocean and atmosphere carbon reservoirs (∼2000 Gt C), as indicated by isotope analyses in the New Jersey sites (Fig. 2) and for surface-dwelling planktonic foraminifera [1,11,13] and terrestrial carbonates [2,59]. This would require only ∼200 Gt of cometary carbon; the equivalent diameter of such a comet with 20–25 wt% carbon [56] and bulk density 1500 kg/m$^3$ [60] would be upwards of 11 km. We emphasize that other factors may have contributed to the magnitude of the surface-ocean/atmosphere $\delta^{13}C$ shift, which would reduce the re-

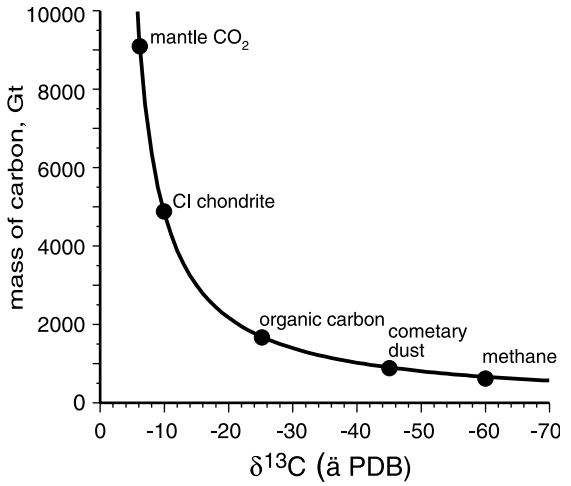


Fig. 8. Mass of carbon as a function of its carbon isotopic composition required to produce a −1‰ shift in the modern total exchangeable ocean–atmosphere carbon reservoir (40 000 Gt; [78,79]). The mass of carbon necessary to cause an isotopic shift in the carbon reservoir is given by:

$$C_a = C_i\left(\frac{\Delta\delta^{13}C}{\delta^{13}C_a-\delta^{13}C_i-\Delta\delta^{13}C}\right)$$

where $C_i$ is the initial mass of carbon of isotopic composition $\delta^{13}C_i$ in the reservoir, $C_a$ is the mass of carbon of isotopic composition $\delta^{13}C_a$ added to the reservoir, and $\Delta\delta^{13}C$ is the change in the $\delta^{13}C$ value of the reservoir. The $\delta^{13}C$ of oceanic dissolved inorganic carbon immediately prior to the CIE was about 1.5‰ [69]; assuming a partitioning between organic and inorganic carbon similar to modern, this indicates an exchangeable carbon isotopic composition of −0.75‰. Nominal carbon isotopic compositions are shown for mantle $CO_2$ [80], CI chondrites [81], organic carbon [80], comets [58], and methane [6] for comparison.

quired comet size. For instance, a ∼2‰ decrease in the $\delta^{13}C$ value of the surface-ocean/atmosphere reservoir at the K/T boundary has been attributed to a reduction in productivity [68]. The convergence of planktonic and benthic foraminiferal $\delta^{13}C$ values suggests that this may also have occurred at the P/E boundary [1,13], in which case only ∼95 Gt of cometary carbon (∼8 km equivalent diameter) would be required to explain the remaining ∼2‰ shift. Given the uncertainties in the properties of comets, impact dynamics and the response of the perturbed carbon reservoir, we believe that ∼10 km for the P/E comet is a plausible estimate and note that modern comets such as P/Halley can be of similar size [61].

The nominal size of the postulated P/E comet is comparable to the K/T bolide (10 ± 4 km) whose size was estimated primarily from the iridium content of the ∼1 cm thick boundary clay [62]. Our suggestion that the P/E impactor was a volatile-rich comet rather than an asteroid could help explain why there is only a small iridium anomaly found associated with the ∼1 cm thick gray layer at Zumaya [14]. Nevertheless, we acknowledge that it is difficult to reconcile the small magnitude of the observed iridium anomaly at Zumaya with the thickness of the presumed ejecta layer using reasonable cometary compositions. For example, if a cometary nucleus contains about equal proportions of carbon and a silicate fraction [60] with a chondritic abundance of ∼500 ppb Ir, the dilution of 100 Gt of chondritic material by a factor of 5000 to produce a 100 ppt Ir anomaly would result in the equivalent of an ejecta layer about 40 cm thick. This is considerably thicker than the gray layer at Zumaya but additional data on iridium contents and detailed lithologic characteristics from other sections are needed to understand the nature of the discrepancy. Interestingly, a similar calculation for a 10 km chondritic asteroid as the K/T impactor (dilution by a factor of 50 to produce a 10 ppb Ir anomaly [63]) results in an ejecta layer of about 5 cm that is appreciably thicker than observed for the K/T boundary clay.

Impacts of large comets are rare but hardly improbable events; the collision rate for comets larger than 10 km is estimated to be about $10^{-8}$ $yr^{-1}$, about a factor of three greater than for >8 km diameter asteroids [64]. We have not identified the site of the postulated P/E impact. However, large impact craters continue to be found on land (e.g. [65]) and, since a larger portion of the Earth's surface area is oceanic rather than continental, it must be acknowledged that the P/E impact may have occurred on oceanic crust. Impact craters of any age have been difficult to find in the ocean basins, although they must exist given the continental crater record [66].

## 6. Contribution from seafloor methane hydrates

Simultaneous mechanical disruption of sedi-

ments and consequent release of methane hydrates could conceivably be triggered by an impact event. Slumping on the continental slope would presumably have occurred coincident with continental shelf impacts such as those that created the 85 km diameter Chesapeake crater of late Eocene age (35 Ma) on the coastal plain of Virginia [65] and the 45 km diameter Montagnais crater of early Eocene age (50.5 Ma) on the Nova Scotia continental shelf [67]. However, no significant negative shift in ocean carbon isotope values has been documented coincident with these events (e.g. [68,69]). This suggests that the amount of methane released as a result of impact-induced slumping was small relative to the whole ocean carbon reservoir, although some release of methane hydrate at the time of impact would be consistent with widespread slumping along the western North Atlantic margin at the time of the CIE [60]).

The highest potential for release of large amounts of seafloor methane hydrate would presumably result from a direct impact in an area of gas hydrate accumulation. At the Blake Ridge, which is thought to be hydrate-rich in comparison to other areas, only $\sim$35 Gt of carbon is present either as hydrate or gas in a 26 000 km$^2$ area [70]. This means that if a large impact activated this entire area (equivalent to a $\sim$180 km diameter crater) the amount of methane that could be released directly would be only a small fraction of that required to produce the initial isotopic decrease at the CIE. On the other hand, greenhouse warming from the introduction of extraterrestrial carbon into the atmosphere may have triggered thermal dissociation of methane.

## 7. Greenhouse warming

The P/E impact hypothesis implies that a cometary body introduced $\sim$100–200 Gt carbon directly into the atmosphere where it would have oxidized to $CO_2$. While there is little agreement on Paleogene atmospheric $CO_2$ levels, a recent estimate suggests that they may have been comparable to present-day levels of $\sim$300 ppm [71], or equivalent to $\sim$600 Gt of carbon. The comet impact hypothesis would therefore imply a virtually instantaneous $\sim$15–30% increase in atmospheric $pCO_2$ and the P/E thermal maximum that occurred synchronous with the CIE is an expected consequence, through greenhouse warming. The massive initial injection of $CO_2$ and resultant greenhouse warming would also have produced newly corrosive and warmer (and hence less oxygenated) bottom waters that have previously been suggested as proximate causal mechanisms for the mass extinction of benthic foraminifera coincident with the CIE [1,4]. Bottom-water warming may also have eventually resulted in thermal dissociation of seafloor gas hydrates, accentuating the environmental and carbon isotopic effects.

## 8. Discussion

To explain the CIE, Dickens et al. [6] excluded mantle $CO_2$ as a realistic source of $^{12}$C-enriched carbon, given its relatively high ($-5$‰) $\delta^{13}$C value compared to the magnitude of the CIE, and argued that methane hydrate with $-60$‰ $\delta^{13}$C was practically the only viable alternative. We have tried to build a case that extraterrestrial carbon is another potential source of light carbon, which can account for the extremely rapid onset of the CIE while consequent dissociation of seafloor methane hydrate may be responsible for the more gradual (over 10s of kyr) and larger ($\sim$2.5‰) decrease in whole-ocean $\delta^{13}$C values. A cometary impact coincident with the P/E boundary can also help explain some enigmatic features associated with this event, such as the iridium anomaly at Zumaya, the abrupt appearance of kaolinitic clays with abundant magnetic nanoparticles on the coastal shelf of NJ, and especially the nearly simultaneous onset of the CIE and the thermal maximum. Indeed, a key feature and testable prediction of a comet impact is that it should produce virtually instantaneous environmental effects in the atmosphere and surface ocean with later repercussions in the deeper ocean.

Recently, a high-resolution isotopic record of the temporal relationship between warming and carbon input was published from Site 690 and

interpreted as showing that the CIE was preceded by a brief period of surface-water warming that somehow led to the thermal dissociation of seafloor methane hydrate [13]. For the following reasons, we suggest that this record instead provides evidence more compatible with the comet impact hypothesis:

1. A decrease of −1.5‰ in $\delta^{18}O$ single-specimen values of surface-dwelling planktonic foraminifera was described as occurring over 3 cm below the virtually instantaneous (within 1 cm) onset of excursion $\delta^{13}C$ values, which is the primary observational basis cited [13] for a thermal precursor to the CIE. However, the data plotted in figure 3 of [13] show that pre-CIE $\delta^{18}O$ values at the top of this 3 cm interval (as indicated by correspondence with pre-CIE $\delta^{13}C$ values) are virtually equivalent to those at the bottom of the interval, so that the variability within this interval seems more likely to reflect normal (interannual to millennial) variations rather than a unidirectional warming as interpreted by [13]. The bimodal distribution of both $\delta^{13}C$ and $\delta^{18}O$ values in the single-specimen stable isotope data at the onset of the CIE (level 2 in [13]) indicates an essentially instantaneous 4‰ decrease in surface-ocean and atmosphere $\delta^{13}C$ values synchronous with a very rapid 6°C increase in surface-water temperature.
2. The cited sequence of first excursion $\delta^{13}C$ values from surface-dwelling to thermocline-dwelling planktonic foraminifera suggests a top-down hydrographic progression of the onset of the CIE. This top-down progression of events is also consistent with inferences drawn from planktonic foraminiferal assemblage changes [72]. Thomas et al. [13] explained the progression of the carbon isotope anomaly from surface to deep waters as due to a rapid transfer of methane from the dissociated hydrates into the surface ocean and atmosphere without first oxidizing near the source in the deep sea. However, experimental data indicate that methane released in the water column above the hydrate stability zone, as would be the case following thermal dissociation, is extremely unlikely to enter the atmosphere prior to oxidation [73]. A simpler explanation follows directly from the comet impact hypothesis, which predicts exactly such a top-down progression because the comet's isotopically light carbon would be injected first into the atmosphere and propagate into the shallow and then deeper ocean. If the comet impact hypothesis is correct, we would expect that the initial input of light carbon and atmosphere/surface-ocean warming occurred simultaneously and virtually instantaneously at the limits of stratigraphic resolution.

## 9. Conclusions

In conclusion, we believe that a comet impact provides a viable and direct method of delivery of $^{12}C$-rich carbon to initiate the CIE and the P/E thermal maximum, which may have triggered a more gradual thermal dissociation of seafloor methane hydrates. The biotic and environmental response to the hypothesized P/E impact, which included the brief dominance of an exotic excursion plankton assemblage [27,28] and a mass extinction among benthic foraminifera [1,4], was clearly different from that following the K/T impact [62], which resulted in massive extinctions of plankton but with little effect on benthic communities [68]. These considerations, together with large impacts that have had little apparent long-term environmental consequences [74], suggest that the effects and signatures of large impacts vary and depend strongly on factors such as the composition of the impactor [75,76] as well as the target area, and Earth's climate state prior to the impact. If supported by further evidence of tracers of extraterrestrial material in CIE deposits, the P/E impact may have implications for the cause of other catastrophic events accompanied by sudden negative carbon isotope excursions, such as at the Permo–Triassic boundary [77].

## Acknowledgements

We thank Marie-Pierre Aubry, Bill Berggren,

Wally Broecker, Julie Carlut, Jeff Gee, Roger Hewins, Mimi Katz, Ken Miller, Paul Olsen and especially Frank Kyte, who pointed out problems with the ejecta mass budget, for useful comments and discussions, and journal reviewers for critical comments that helped us to refine our ideas and improve the manuscript. This work was supported by grant OCE 0084032 (Biocomplexity) from the U.S. National Science Foundation and a NSF Graduate Research Fellowship (B.S.C.). LDEO #6449.*[BARD]*

## References

[1] J.P. Kennett, L.D. Stott, Abrupt deep-sea warming, palaeoceanographic changes and benthic extinctions at the end of the Palaeocene, Nature 353 (1991) 225–229.

[2] P.L. Koch, J. Zachos, P.D. Gingerich, Correlation between isotope records in marine and continental carbon reservoirs near the Palaeocene/Eocene boundary, Nature 358 (1992) 319–322.

[3] J.C. Zachos, K.C. Lohmann, J.C.G. Walker, S.W. Wise, Abrupt climate change and transient climates during the Paleogene: A marine perspective, J. Geol. 101 (1993) 191–213.

[4] E. Thomas, N.J. Shackleton, The Paleocene-Eocene benthic foraminiferal extinction and stable isotope anomalies, in: R.W.O.B. Knox, R.M. Corfield, R.E. Dunay (Eds.), Correlation of the Early Paleogene in Northwest Europe, Geol. Soc. London Spec. Publ. 101, 1996, pp. 401–441.

[5] M.C. Maas, M.R.L. Anthony, P.D. Gingerich, G.F. Gunnell, D.K. Krause, Mammalian generic diversity and turnover in the late Paleocene and early Eocene of the Bighorn and Crazy Mountains Basins, Wyoming and Montana, Palaeogeogr. Palaeoclimatol. Palaeoecol. 115 (1995) 181–207.

[6] G.R. Dickens, J.R. O'Neil, D.K. Rea, R.M. Owen, Dissociation of oceanic methane hydrate as a cause of the carbon isotope excursion at the end of the Paleocene, Paleoceanography 10 (1995) 965–971.

[7] G.R. Dickens, M.M. Castillo, J.C.G. Walker, A blast of gas in the latest Paleocene: Simulating first-order effects of massive dissociation of oceanic methane hydrate, Geology 25 (1997) 259–262.

[8] K. Kaiho, T. Arinobu, R. Ishiwatari, H.E.G. Morgans, H. Okada, N. Takeda, K. Tazaki, G. Zhou, Y. Kajiwara, R. Matsumoto, A. Hirai, N. Niitsuma, H. Wada, Latest Paleocene benthic foraminiferal extinction and environmental changes at Tawanui, New Zealand, Paleoceanography 11 (1996) 447–465.

[9] M.E. Katz, B.S. Cramer, G.S. Mountain, S. Katz, K.G. Miller, Uncorking the bottle: What triggered the Paleocene/Eocene thermal maximum methane release?, Paleoceanography 16 (2001) 549–562.

[10] T.J. Bralower, D.J. Thomas, J.C. Zachos, M.M. Hirschmann, U. Rohl, H. Sigurdsson, E. Thomas, D.L. Whitney, High-resolution records of the late Paleocene thermal maximum and circum-Caribbean volcanism: Is there a causal link?, Geology 25 (1997) 963–966.

[11] D.J. Thomas, T.J. Bralower, J.C. Zachos, New evidence for subtropical warming during the late Paleocene thermal maximum: Stable isotopes from Deep Sea Drilling Project Site 527, Walvis Ridge, Paleoceanography 14 (1999) 561–570.

[12] S. Bains, R.M. Corfield, R.D. Norris, Mechanism of climate warming at the end of the Paleocene, Science 285 (1999) 724–727.

[13] D.J. Thomas, J.C. Zachos, T.J. Bralower, E. Thomas, S. Bohaty, Warming the fuel for the fire: Evidence for the thermal dissociation of methane hydrate during the Paleocene-Eocene thermal maximum, Geology 30 (2002) 1067–1070.

[14] B. Schmitz, F. Asaro, E. Molina, S. Monechi, K. von Salis, R.P. Speijer, High-resolution iridium, $\delta^{13}C$, $\delta^{18}O$, foraminifera and nannofossil profiles across the latest Paleocene benthic extinction event at Zumaya, Spain, Palaeogeogr. Palaeoclimatol. Palaeoecol. 133 (1997) 49–68.

[15] T. Dolenec, J. Pavsic, S. Lojen, Ir anomalies and other elemental markers near the Palaeocene-Eocene boundary in a flysch sequence for the Western Tethys (Slovenia), Terra Nova 12 (2001) 199–204.

[16] K.G. Miller, P.J. Sugarman, J.V. Browning, R.K. Olsson, S.F. Pekar, T.J. Reilly, B.S. Cramer, M.-P. Aubry, R.P. Lawrence, J. Curran, M. Stewart, J.M. Metzger, J. Uptegrove, D. Bukry, L.H. Burckle, J. D.Wright, M.D. Feigenson, G.J. Brenner, R.F. Dalton, Bass River Site, in: K.G. Miller, P.J. Sugarman, J.V. Browning (Eds.), Proc. ODP Init. Reports 174AX (1998) 5–43.

[17] B.S. Cramer, M.-P. Aubry, K.G. Miller, R.K. Olsson, J.D. Wright, D.V. Kent, An exceptional chronologic, isotopic, and clay mineralogic record of the latest Paleocene thermal maximum, Bass River, NJ, ODP 174AX, Bull. Soc. Geol. France 170 (1999) 883–897.

[18] K.G. Miller, P.J. Sugarman, J.V. Browning, B.S. Cramer, R.K. Olsson, L.d. Romero, M.-P. Aubry, S.F. Pekar, M.D. Georgescu, K.T. Metzger, D.H. Monteverde, E.S. Skinner, J. Uptegrove, L.G. Mullikin, F.L. Muller, M.D. Feigenson, T.J. Reilly, G.J. Brenner, D. Queen, Ancora site report, in: K.G. Miller, P.J. Sugarman, J.V. Browning (Eds.), Proc. ODP Init. Reports 174AX (1998) http://www-odp.tamu.edu/publications/174AXSIR/VOLUME/CHAPTERS/174AXS-1.PDF.

[19] L. Lanci, D.V. Kent and K.G. Miller, Detection of sequence boundaries using core-log integration of magnetic susceptibility and natural gamma-ray measurements at the Ancora site on the Atlantic Coastal Plain, J. Geophys. Res. 107 (2002) 2216, 10.1029/2000JB000026.

[20] T.G. Gibson, L.M. Bybell, D.B. Mason, Stratigraphic and climatic implications of clay mineral changes around the

Paleocene/Eocene boundary of the northeastern US margin, Sediment. Geol. 134 (2000) 65–92.
[21] M.-P. Aubry, Where should the Global Stratotype Section and Point (GSSP) for the Paleocene/Eocene boundary be located?, Bull. Soc. Geol. France 171 (2000) 461–476.
[22] M.-P. Bolle, T. Adatte, G. Keller, K. von Salis, S. Burns, The Paleocene-Eocene transition in the southern Tethys (Tunisia): Climatic and environmental fluctuations, Bull. Soc. Geol. France 170 (1999) 661–680.
[23] C. Robert, J.P. Kennett, Antarctic subtropical humic episode at the Paleocene-Eocene boundary: Clay-mineral evidence, Geology 22 (1994) 211–214.
[24] M. Thiry, Palaeoclimatic interpretation of clay minerals in marine deposits: An outlook from the continental origin, Earth Sci. Rev. 49 (2000) 201–221.
[25] U. Röhl, T.J. Bralower, R.D. Norris, G. Wefer, New chronology for the late Paleocene thermal maximum and its environmental implications, Geology 28 (2000) 927–930.
[26] M.-P. Aubry, B.S. Cramer, K.G. Miller, J.D. Wright, D.V. Kent, R.K. Olsson, Late Paleocene event chronology unconformities, not diachrony, Bull. Soc. Geol. France 171 (2000) 367–378.
[27] D.C. Kelly, T.J. Bralower, J.C. Zachos, I. Premoli-Silva, E. Thomas, Rapid diversification of planktonic foraminifera in the tropical Pacific (ODP Site 865) during the late Paleocene thermal maximum, Geology 24 (1996) 423–426.
[28] M.P. Aubry, A. Sanfilippo, Late Paleocene-Early Eocene sedimentary history in western Cuba: Implications for the LPTM and for regional tectonic history, Micropaleontology 45 (1999) 5–18.
[29] B.S. Cramer, K.G. Miller, J.D. Wright, M.-P. Aubry, R.K. Olsson, Neritic records of the late Paleocene thermal maximum from New Jersey, GFF 122 (2000) 38–39.
[30] D.J. Dunlop, Superparamagnetic and single-domain threshold sizes in magnetite, J. Geophys. Res. 78 (1973) 1780–1793.
[31] M. Winklhofer, K. Fabian, F. Heider, Magnetic blocking temperatures of magnetite calculated with a three-dimensional micromagnetic model, J. Geophys. Res. 102 (1997) 22695–22710.
[32] A.J. Newell, R.T. Merrill, Size dependence of hysteresis properties of small pseudo-single-domain grains, J. Geophys. Res. 105 (2000) 19393–19403.
[33] L. Tauxe, T.A.T. Mullender, T. Pick, Potbellies, wasp-waists, and superparamagnetism in magnetic hysteresis, J. Geophys. Res. 101 (1996) 571–583.
[34] L. Lanci, D.V. Kent, Introduction of thermal activation in forward modeling of SD hysteresis loops and implications for the interpretation of the Day diagrams, J. Geophys. Res. 108 (B3) (2002) 10.1029/2001JB000944.
[35] D.J. Dunlop, Theory and application of the Day plot ($M_{rs}/M_s$ versus $H_{cr}/H_c$) 2. Application to data for rocks, sediments, and soils, J. Geophys. Res. 107 (2002) 10.129/2001JB000487.
[36] A.V. Smirnov, J.A. Tarduno, Low-temperature magnetic properties of pelagic sediments (Ocean Drilling Project Site 805C): Tracers of maghemitization and magnetic mineral reduction, J. Geophys. Res. 105 (2000) 16457–16471.
[37] K. Fukuma, M. Torii, Variable shape of magnetic hysteresis loops in the Chinese loess-paleosol sequence, Earth Planets Space 50 (1998) 9–14.
[38] S.T. Brachfeld, S.K. Banerjee, A new high-resolution geomagnetic relative paleointensity record for the North American Holocene: A comparison of sedimentary and absolute intensity data, J. Geophys. Res. 105 (2000) 821–834.
[39] J. King, S.K. Banerjee, J. Marvin, O. Ozdemir, A comparison of different magnetic methods for determining the relative grain size of magnetite in natural materials; some results from lake sediments, Earth Planet. Sci. Lett. 59 (1982) 404–419.
[40] J.E.T. Channell, C. McCabe, Comparison of magnetic hysteresis parameters of remagnetized and unremagnetized limestones, J. Geophys. Res. 99 (1994) 4613–4623.
[41] S.-B.R. Chang, J.L. Kirschvink, Magnetofossils, the magnetization of sediments, and the evolution of magnetite biomineralization, Annu. Rev. Earth Planet. Sci. 17 (1989) 169–195.
[42] B.M. Moskowitz, R.B. Frankel, P.J. Flanders, R.P. Blakemore, B.B. Schwartz, Magnetic properties of magnetotactic bacteria, J. Magn. Magn. Mater. 73 (1988) 273–288.
[43] R. Karlin, M. Lyle, G.R. Heath, Authigenic magnetite formation in suboxic marine sediments, Nature 326 (1987) 490–493.
[44] B.W. Leslie, S.P. Lund, D.E. Hammond, Rock magnetic evidence for the dissolution and authigenic growth of magnetic minerals within anoxic marine sediments of the California continental borderland, J. Geophys. Res. 95 (1990) 4437–4452.
[45] J.A. Tarduno, Temporal trends of magnetic dissolution in the pelagic realm: Gauging paleoproductivity?, Earth Planet. Sci. Lett. 123 (1994) 39–48.
[46] T.J. Wdowiak, L.P. Armendarez, D.G. Agresti, M.L. Wade, S.Y. Wdowiak, P. Claeys, G. Izett, Presence of an iron-rich nanophase material in the upper layer of the Cretaceous-Tertiary boundary clay, Meteorit. Planet. Sci. 36 (2001) 123–133.
[47] H.C. Verma, C. Upadhyay, R.P. Tripathi, A. Tripathi, A.D. Shukla, N. Bhandari, Nano-sized iron phases at the K/T and P/T boundaries revealed by Mössbauer spectroscopy, Lunar Planet. Sci. 32 (2001) 1270.pdf.
[48] B. Schmitz, F. Asaro, Iridium geochemistry of volcanic ash layers from the early Eocene rifting of the northeastern North Atlantic and some other Phanerozoic events, Geol. Soc. Am. Bull. 108 (1996) 489–504.
[49] G. Ravizza, R.N. Norris, J. Blusztajn, M.-P. Aubry, An osmium isotope excursion associated with the late Paleocene thermal maximum: Evidence of intensified chemical weathering, Paleoceanography 16 (2001) 155–163.
[50] W.J. Pegram, K.K. Turekian, The osmium isotopic composition change of Cenozoic sea water as inferred from a

deep-sea core corrected for meteoritic contributions, Geochim. Cosmochim. Acta 63 (1999) 4053–4058.
[51] K.G. Miller, T.R. Janecek, M.E. Katz, D.J. Keil, Abyssal circulation and benthic foraminiferal changes near the Paleocene/Eocene boundary, Paleoceanography 2 (1987) 741–761.
[52] K.A. Farley, Cenozoic variations in the flux of interplanetary dust recorded by $^{3}$He in a deep-sea sediment, Nature 376 (1995) 153–156.
[53] F.T. Kyte, J.T. Wasson, Accretion rate of extraterrestrial matter: Iridium deposited 33 to 67 million years ago, Science 232 (1986) 1225–1229.
[54] K.A. Farley, A. Montanari, R.M. Shoemaker, C.S. Shoemaker, Geochemical evidence for a comet shower in the late Eocene, Science 280 (1998) 1250–1253.
[55] A.H. Delsemme, The chemistry of comets, Philos. Trans. R. Soc. London A 325 (1988) 509–523.
[56] E.K. Jessberger, J. Kissel, Chemical properties of cometary dust and a note on carbon isotopes, in: R.L. Newburn, M. Neugebauer, J.H. Rahe (Eds.), Comets in the Post-Halley Era, vol. 2, Kluwer Academic, Amsterdam, 1991, pp. 1075–1092.
[57] E.K. Jessberger, Rocky cometary particulates: Their elemental, isotopic and mineralogical ingredients, Space Sci. Rev. 90 (1999) 91–97.
[58] S. Messenger, Identification of molecular-cloud material in interplanetary dust particles, Nature 404 (2000) 968–971.
[59] G.J. Bowen, P.L. Koch, P.D. Gingerich, R.D. Norris, S. Bains, R.M. Corfield, Refined isotope stratigraphy across the continental Paleocene-Eocene boundary on Polecat Bench in the northern Bighorn Basin, in: P.D. Gingerich (Ed.), Paleocene-Eocene Stratigraphy and Biotic Change in the Bighorn and Clarks Fork Basins, Wyoming, University of Michigan Papers on Paleontology No. 33, Museum of Paleontology, The University of Michigan, Ann Arbor, MI, 2001, pp. 73–88.
[60] J.M. Greenberg, Making a comet nucleus, Astron. Astrophys. 330 (1998) 375–380.
[61] K. Lodders, B. Fegley, Jr., The Planetary Scientist's Companion, Oxford University Press, New York, 1998, 371 pp.
[62] L.W. Alvarez, W. Alvarez, F. Asaro, H.V. Michel, Extraterrestrial cause for the Cretaceous-Tertiary extinction, Science 208 (1980) 1095–1108.
[63] F.T. Kyte, Tracers of the extraterrestrial component in sediments and inferences for Earth's accretion history, Geol. Soc. Am. Spec. Paper 356 (2002) 21–38.
[64] E.M. Shoemaker, R.F. Wolfe, C.S. Shoemaker, Asteroid and comet flux in the neighborhood of Earth, in: V.L. Sharpton, P.D. Ward (Eds.), Global Catastrophes in Earth History, Geol. Soc. Am. Spec. Paper 247 (1990) 155–170.
[65] C.W. Poag, D.S. Powars, L.J. Poppe, R.B. Mixon, Meteoroid mayhem in Ole Virginny Source of the North American tektite strewn field, Geology 22 (1994) 691–694.
[66] R.A.F. Grieve, Extraterrestrial impact events the record in the rocks and the stratigraphic column, Palaeogeogr. Palaeoclimatol. Palaeoecol. 132 (1997) 5–23.
[67] L.F. Jansa, G. Pe-Piper, P.B. Robertson, O. Friedenreich, Montagnais: A submarine impact structure on the Scotian Shelf, Eastern Canada, Geol. Soc. Am. Bull. 101 (1989) 450–463.
[68] S. D'Hondt, P. Donaghay, J.C. Zachos, D. Luttenberg, M. Lindinger, Organic carbon fluxes and ecological recovery from the Cretaceous-Tertiary mass extinction, Science 282 (1998) 276–279.
[69] J. Zachos, M.N. Pagani, L. Sloan, E. Thomas, K. Billups, Trends, rhythms, and aberrations in global climate 65 Ma to present, Science 292 (2001) 686–693.
[70] G.R. Dickens, C.K. Paull, P. Wallace, Scientific Party ODP, Direct measurement of in situ methane quantities in a large gas-hydrate reservoir, Nature 385 (1997) 426–428.
[71] D.L. Royer, S.L. Wing, D.J. Beerling, D.W. Jolley, P.L. Koch, L.J. Hickey, R.A. Berner, Paleobotanical evidence for near present-day levels of atmospheric $CO_2$ during part of the Tertiary, Science 292 (2001) 2310–2313.
[72] D.C. Kelly, Response of Antarctic (ODP Site 690) planktonic foraminifera to the Paleocene-Eocene thermal maximum: Faunal evidence for ocean/climate change, Paleoceanography 17 (2002) 23/1–23/13.
[73] G. Rehder, P.W. Brewer, E.T. Peltzer, G. Friederich, Enhanced lifetime of methane bubble streams within the deep ocean, Geophys. Res. Lett. 29 (2002) 10.1029/2001GL013966.
[74] C.W. Poag, Roadblocks on the kill curve: Testing the Raup hypothesis, Palaios 12 (1997) 582–590.
[75] P. Wilde, M.S. Quinby-Hunt, Collisions with ice/volatile objects: Geological implications - a qualitative treatment, Palaeogeogr. Palaeoclimatol. Palaeoecol. 132 (1997) 47–63.
[76] D. Deming, On the possible influence of extraterrestrial volatiles on Earth's climate and the origin of the oceans, Palaeogeogr. Palaeoclimatol. Palaeoecol. 246 (1999) 33–51.
[77] Y.G. Jin, Y. Wang, W. Wang, Q.H. Shang, C.Q. Cao, D.H. Erwin, Pattern of marine mass extinction near the Permian-Triassic boundary in south China, Science 289 (2000) 432–436.
[78] W.S. Broecker, T.-H. Peng, What caused the glacial to interglacial $CO_2$ change?, in: M. Heimann (Ed.), The Global Carbon Cycle, NATO ASI Series I, no. 15, 1993, pp. 95–115.
[79] U. Siegenthaler, Modeling the present-day oceanic carbon cycle, in: M. Heimann (Ed.), The Global Carbon Cycle, NATO ASI Series I, no. 15, 1993, pp. 367–395.
[80] G. Faure, Principles of Isotope Geology, Wiley, New York, 1986, 589 pp.
[81] J.F. Kerridge, Carbon, hydrogen and nitrogen in carbonaceous chondrites: Abundances and isotopic compositions in bulk samples, Geochim. Cosmochim. Acta 49 (1985) 1707–1714.